

Enhancing superconductivity using thermal bosons

Ekaterina Vlasiuk,¹ Manfred Salmhofer,¹ Eugene Demler,² and Richard Schmidt¹

¹*Institute for Theoretical Physics, Heidelberg University, 69120 Heidelberg, Germany*

²*Institute for Theoretical Physics, ETH Zürich, 8093 Zürich, Switzerland*

We investigate how the strong coupling of a superconductor to thermal bosons can enhance its superconducting critical temperature. To tackle this problem, we use a renormalization group approach that allows us to describe the competition between density fluctuations and the build-up of boson-induced attraction between fermions. Capturing the mutual influence of bosonic and fermionic sectors, the self-consistent renormalization group framework predicts a robust increase of the critical temperature across a wide range of interactions. We find a nontrivial dependence of the critical temperature on the boson mass and we establish a phase diagram for enhanced superconductivity driven by bosons being either in the condensed or thermal state. We outline possible experimental realizations in cold atomic systems and discuss implementations using electron-exciton mixtures in van der Waals material heterostructures.

What are possible ways to increase the critical temperature T_c of a superconductor? Are there bounds on T_c and what defines them? Can bounds be changed by coupling the superconductor (SC) to a separate many-body system that may or may not be in a quantum degenerate state? These are among the questions that have recently come into focus driven by theory [1–3] and experimental progress alike [4–7]. In this letter, we consider these questions by studying how the critical temperature of a generic superconductor reacts to the coupling to a thermal bosonic medium. In particular we explore how a significant enhancement of T_c can be achieved when entering the strong-coupling regime, where electrons may form bound states with the bosons, such as realized in two-dimensional (2D) materials [8] or synthetic quantum matter [9, 10].

We focus on two aspects, namely whether a purely thermal medium can enhance T_c , and whether it is possible to transition from one mechanism producing a bound on T_c to another. To gain intuition, consider a phonon-mediated superconductor: here the Debye energy acts as the natural scale that limits T_c [2]. But what happens if one couples this superconductor to an additional species of particles? The question then arises whether the superconductor’s internal bound on T_c is still the relevant one, or if there is a transition to another bound associated with the scales intrinsic to the newly-introduced medium.

While qualitative proposals for exciton-mediated superconductors [11, 12] have existed for a long time, in recent years modifications to boson-induced superconductivity came into focus in cold atoms [13] and 2D materials [14]. In transition metal dichalcogenides (TMDs) strongly bound excitons [15, 16] in the condensed phase play the role of bosons, mediating the interaction between fermions, similar to phonon exchange in BCS theory [14, 17–19]. Early quantitative investigations have focused on induced superconductivity in analogy to phonon exchange [13, 14, 17]. Later, it was realized that bound state physics between bosons and fermions requires to

go beyond such conventional models [20–22]. It was found that these strongly-coupled systems can induce superconductivity at high dimensionless temperatures T_c/T_F , accompanied by an emergent BCS-BEC crossover in which the Fermi temperature T_F sets a new bound on T_c [20, 23]. In this case, the presence of the coherence in the Bose-Einstein condensate (BEC) of bosons played an essential role, guaranteeing strong mediated forces in the fermionic system. However, one may ask what happens if the bosons become thermal and the thermal de Broglie wavelength becomes comparable to the size of Cooper pairs. Importantly, if the thermal bosons are coupled to an already established s-wave superconductor, will they disrupt the formation of Cooper pairs [24, 25] or enhance their stability [26–28]?

In this letter, we tackle these questions using a Functional Renormalization Group (FRG) approach [29–36]. This allows us to consider the regime of non-perturbative boson-fermion interactions, where the absence of a clear scale separation poses a theoretical challenge, requiring to handle fermion-fermion and boson-fermion interactions on equal footing. We find that accounting for the

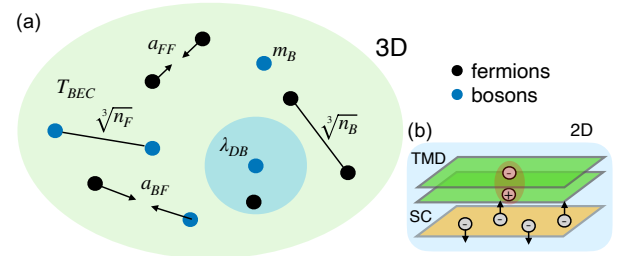


FIG. 1. Platforms for thermal-boson enhanced superconductivity. a) Ultracold atomic Bose-Fermi mixture in three dimensions. Black (blue) dots depict fermions (bosons), and relevant scales of the model are illustrated. b) 2D material heterostructure where interlayer excitons in a transition metal dichalcogenide (TMD) bilayer interact with electrons in a superconducting layer, allowing the formation of an interlayer trion (exciton-electron) bound state.

competition and interplay between bosonic and fermionic degrees of freedom is key to understand the enhancement of T_c due to thermal bosons. We perform the calculations assuming a BCS state for the underlying superconductor, compare the critical temperature with and without the addition of bosons, and we establish a phase diagram of enhanced superconductivity for bosons being in either a thermal or condensed state.

Model.—Having in mind experimental realizations in both cold atoms and van der Waals materials, we consider two-component fermions $\hat{c}_{\sigma\mathbf{k}}^\dagger$ of spin σ and momentum \mathbf{k} , interacting with themselves and with bosonic particles $\hat{b}_{\mathbf{k}}^\dagger$ via attractive, contact interactions of strength g and λ , respectively (see Fig. 1). We assume no interaction between the thermal bosons, resulting in the Hamiltonian ($\sigma = \uparrow, \downarrow$, units $\hbar = k_B = 1$)

$$H = \sum_{\sigma, \mathbf{k}} \varepsilon_{\mathbf{k}}^c \hat{c}_{\sigma\mathbf{k}}^\dagger \hat{c}_{\sigma\mathbf{k}} + \sum_{\mathbf{k}} \varepsilon_{\mathbf{k}}^b \hat{b}_{\mathbf{k}}^\dagger \hat{b}_{\mathbf{k}} + \sum_{\mathbf{p}, \mathbf{q}} \left[g \hat{c}_{\uparrow\mathbf{p}+\mathbf{q}}^\dagger \hat{c}_{\downarrow\mathbf{k}-\mathbf{q}}^\dagger \hat{c}_{\downarrow\mathbf{k}} \hat{c}_{\uparrow\mathbf{p}} + \sum_{\sigma} \lambda^\sigma \hat{c}_{\sigma\mathbf{p}+\mathbf{q}}^\dagger \hat{b}_{\mathbf{k}-\mathbf{q}}^\dagger \hat{b}_{\mathbf{k}} \hat{c}_{\sigma\mathbf{p}} \right], \quad (1)$$

with $\varepsilon_{\mathbf{k}}^{c,b} = \mathbf{k}^2/2m_{F,B} - \mu_{F,B}$. We consider $SU(2)$ fermions with $m_F^c \equiv m_F$; μ_F and μ_B are the chemical potentials of fermions and bosons, determined by the corresponding densities n_F and n_B at given temperature T . In absence of the coupling to the bosons, Eq. (1) gives rise to the BCS-BEC crossover, as $g < 0$ is varied from weak to strong coupling [37–39]. The coupling $\lambda^\sigma < 0$ leads to a modification of T_c due to the presence of bosons. While in the following we focus on the three-dimensional setting, the extension of our approach to two dimensions is straightforward, and we expect such an analysis to yield qualitatively similar results.

In this work we study how the BCS state is modified by the presence of thermal bosons. Already in the simplifying BCS limit, the system is governed by an interplay of various scales (Fig. 1a) that feature no clear scale separation: a) the interparticle distances set by the densities n_F and n_B ; b) the scattering length between fermions a_{FF} , and between bosons and fermions a_{BF} ; and c) the thermal de Broglie wavelength λ_{DB} beyond which bosons lose their quantum coherence. All these scales are related by the particles' masses m_F and m_B . For concreteness, in most numerical results we focus on the mass ratio $m_B/m_F = 2.175$ realized in a K^{40} -Rb 87 Bose-Fermi mixture, and which is also close to typical mass ratios in exciton-electron mixtures.

Method.—In order to analyze a system lacking scale separation, we take advantage of the functional RG (FRG). In contrast to many functional approaches [40, 41], the FRG allows one to incorporate bosonic and fermionic fluctuations on equal footing. The central ob-

ject of the FRG is the Wetterich flow equation [35]

$$\partial_k \Gamma_k = \frac{1}{2} \text{STr} \left(\frac{1}{\Gamma_k^{(2)} + R_k} \partial_k R_k \right). \quad (2)$$

Here k is the RG scale, and the effective flowing action Γ_k is a functional of the fields of the theory. Its second order functional derivative $\Gamma_k^{(2)}$ is regulated by the function R_k . The symbol STr denotes the summation over momenta \mathbf{p} , Matsubara frequencies ω_n , and all fields with the appropriate minus signs for fermions.

In order to establish the basis for our analysis, we briefly discuss the critical behaviour of the isolated interacting fermionic gas, governed by the BCS-BEC crossover. BCS theory [42] within Leggett's approach provides a useful approximation of the crossover up to moderate interaction strength [43, 44]. In order to reproduce the corresponding critical temperature using the FRG [45], we utilize the truncation of the effective action

$$\Gamma_k^{BCS} = - \sum_{\sigma=\uparrow,\downarrow} \int_P \psi_\sigma^*(P) \left(i\omega_n - \frac{\mathbf{p}^2}{2m_F} + \mu_F \right) \psi_\sigma(P) + g_k \int_{QPP'} \psi_\uparrow^*(P+Q) \psi_\downarrow^*(P'-Q) \psi_\downarrow(P') \psi_\uparrow(P), \quad (3)$$

with $\int_P = T \sum_{i\omega_n} \int d^3\mathbf{p}$ and $P = (\omega_n, \mathbf{p})$ and fermionic fields ψ . Using sharp momentum regulators, the regularized fermionic Green's function $(G_F^c)^{-1} = (G_F^c)^{-1} + R_F$ takes the form $G_F^c(\mathbf{p}, \omega) = G_F(\mathbf{p}, \omega) \theta(|\mathbf{p}^2/2m_F - \mu_F| - k^2/2m_F)$. From Eq. (2) one obtains the RG equation $\partial_k g_k = -g_k^2 \tilde{\partial}_k \int_Q G_F^c(Q) G_F^c(-Q)$ diagrammatically represented in Fig. 2(a). The derivative $\tilde{\partial}_k$ acts only on the regulator, i.e. $\tilde{\partial}_k = (\partial_k R_k) \partial_{R_k}$; for details see [46].

Having obtained the RG flow for the BCS state, we next include the coupling to the bosonic sector represented by the field φ . To this end, we use the truncation

$$\Gamma_k = \Gamma_k^{BCS} - \int_P \varphi^*(P) \left(i\omega_n - \frac{\mathbf{p}^2}{2m_B} + \mu_B \right) \varphi(P) + \sum_{\sigma} \lambda_k^\sigma \int_{QPP'} \psi_\sigma^*(P+Q) \varphi^*(P'-Q) \varphi(P') \psi_\sigma(P), \quad (4)$$

as a minimal model that captures the essential physics using flowing coupling constants g_k and λ_k^σ . For example, this truncation does not account for self-energy corrections. However, for density-imbalanced systems featuring thermal bosons their effect is expected to be subleading as also recently observed in cold atom experiments [47].

The fully interacting many-body system is described by the coupled set of RG equations [48] (see Fig. 2(a))

$$\partial_k g_k = -g_k^2 I_{BCS} - \lambda_k^\uparrow \lambda_k^\downarrow I_1, \quad (5)$$

$$\partial_k \lambda_k^\sigma = -\lambda_k^{\sigma 2} (I_3 + I_4) + g_k \lambda_k^{-\sigma} I_2, \quad (6)$$

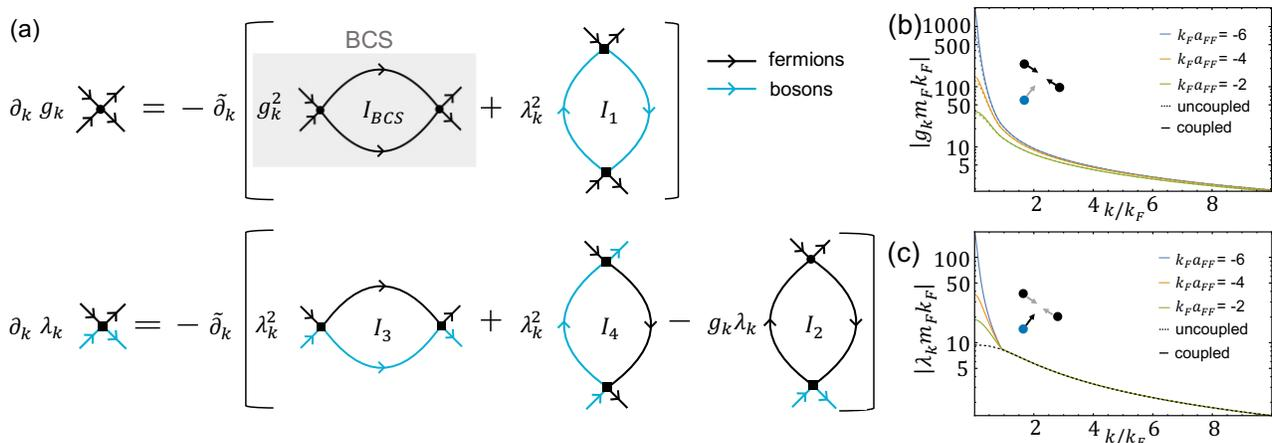


FIG. 2. **Renormalization group analysis.** (a) Diagrammatic representation of the RG equations. Black (blue) lines denote fermionic (bosonic) propagators. (b,c) RG flow with RG scale k of the coupling constants g_k and λ_k with $n_B/n_F = 0.1$, $(k_F a_{BF})^{-1} = -0.2$, $T/T_F = 0.4$, $m_B/m_F = 2.175$. Solid curves represent the self-consistent solution, while dashed curves show the non-selfconsistent flow ($I_1 = 0$ and $I_2 = 0$ in (a)).

where $-\sigma$ denotes the opposite spin of σ . The expressions for I_1, \dots, I_4 , and I_{BCS} depend on temperature T ; for their explicit form see Ref. [46]. In the following, we assume $\lambda^\uparrow = \lambda^\downarrow = \lambda$. As in the BCS analysis, we take into account that the relevant physics occurs at the Fermi surface by projection of momenta onto the Fermi surface at zero center-of-mass momentum. The initial conditions in the UV limit are set by the solution of the Lippmann-Schwinger equation [46].

The critical SC temperature T_c is determined by the divergence of the vertex g_k in the IR limit at $k = 0$, i.e. we employ the Thouless criterion $g_{k=0}^{-1}|_{T=T_c} = 0$. Numerical results for the RG flow of the vertex functions are shown Fig. 2(b,c) at $T > T_c$, for different choices of $(k_F a_{FF})^{-1}$. Comparing the flow of the vertices g , λ in the absence and presence of the coupling between the two RG equations, one observes that the system is governed by the mutual influence of Fermi-Fermi (FF) and Bose-Fermi (BF) correlations. Indeed, due to the coupling with bosons the flow of the pairing vertex g is modified in a non-linear way by the second term in Eq. (5). Similarly, the boson-fermion pairing vertices λ is modified by the fermionic sector. The associated terms I_1 and I_2 describe density fluctuations, and we find that the coupling between bosons and fermions enhances the attractive correlations between fermions, and between bosons and fermions alike (see illustrations in Fig. 2(b,c)).

We have verified the attractive nature of the induced interactions by comparing our result to a weak-coupling effective theory obtained by integrating out the bosons [46]. Moreover, we find that the diagram I_4 — which represents particle exchange and acts analogously to Gorkov corrections — only results in a small modification of interactions. We note that a leading divergence of λ_k , which would signal the formation of fermionic

molecules comprised of a boson and a fermion as the new ground state of the system (i.e. trions in the context of 2D materials), does not occur. SC is thus indeed the dominating instability in our model.

Results.—In Fig. 3(a) the behavior of T_c is shown in absence (dashed blue) and presence of bosons (red and green solid) at fixed density n_B . Answering the first question raised in this work, we find that the critical temperature significantly increases when thermal bosons are added to the system. This increase of T_c is robust across the whole range of fermionic scattering length a_{FF} . The enhancement of T_c by thermal bosons is, however, suppressed as the original superconductor approaches its own bound on T_c/T_F close to the unitary limit. This finding is crucial as it implies that the bound $T_c/T_F \approx 0.16$ [49–51] in the BEC-BCS crossover cannot be exceeded by coupling fermions to a thermal bosonic bath, answering the second question outlined in the beginning of this work.

Analyzing results as in Fig. 3(a) we can construct the ‘phase diagram’ of boson-modified superconductivity shown in Fig. 3(b). We parametrize the phase diagram using two equivalent measures, chosen for easy comparison with experiments in cold atoms and 2D materials [52]. The FF interaction strength is, e.g., expressed in terms of $(k_F a_{FF})^{-1}$ known from Feshbach resonance analysis in cold atoms [53], as well as the zero-temperature SC gap Δ_0 which is readily measurable in solid-state systems. Similarly, we give the BF interaction strength as function of $(k_F a_{BF})^{-1}$ as well as the scattering phase shift δ_{BF} [54], which has been characterized for exciton-electron mixtures and can be readily connected to trion binding energies [55–58].

We identify three phases as function of the Bose-Fermi and Fermi-Fermi interaction strengths. First, the

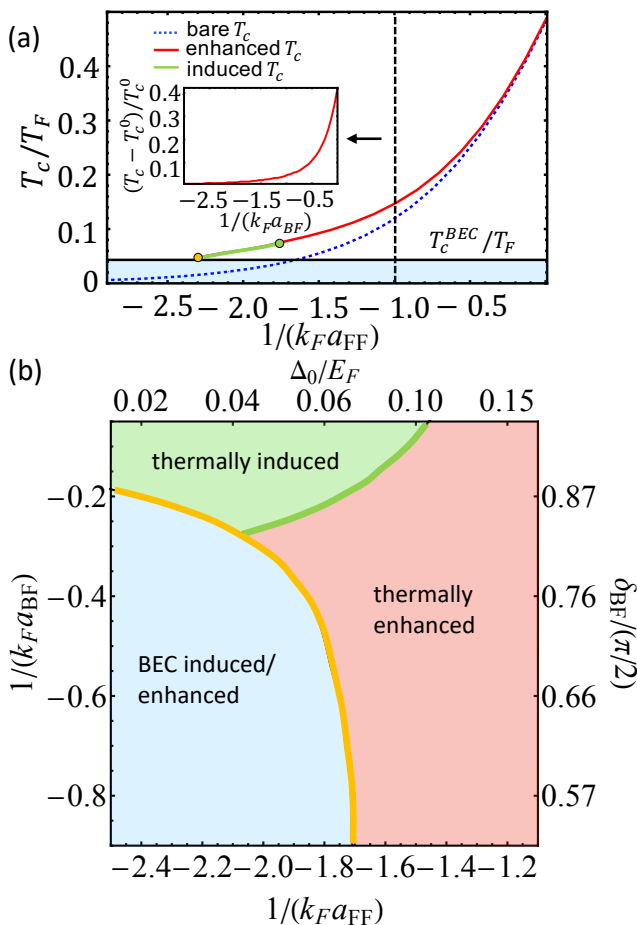


FIG. 3. **Thermal-boson enhanced superconductivity.** (a) Critical temperature T_c/T_F as function of $1/(k_F a_{FF})$ at fixed boson density (solid green and red), compared to the case where bosons are absent (dashed blue). The black line shows the temperature of Bose-Einstein condensation T_c^{BEC} . Parameters are $(k_F a_{BF})^{-1} = -0.2$, $n_B/n_F = 0.1$, $m_B/m_F = 2.175$. Inset: Dependence of T_c on $(k_F a_{BF})^{-1}$ at $(k_F a_{FF})^{-1} = -1$. (b) Phase diagram of boson-modified superconductivity for a Bose-Fermi mixture as in (a). The border between the thermally induced and enhanced superconductivity is determined by the condition $T_c = 2T_c^0$.

weak coupling regime is governed by a phase which requires bosons to be in the superfluid state to enhance SC (shaded blue). Here the system only turns superconducting at temperatures below T_c^{BEC} of Bose condensation, i.e. for $T < T_c^{BEC} \approx 3.3 n_B^{2/3}/m_B$ for an ideal Bose gas in 3D (black solid line in Fig. 3(a)).

At strong coupling $1/(k_F a_{FF}) \gtrsim -1.7$, but intermediate values of $k_F a_{BF}$, the modified T_c raises above T_c^{BEC} . Here thermal bosons are sufficient to enhance SC (shaded red in Fig. 3(b)). At large BF interactions, we find that the thermal bosons provide the dominant mechanism driving SC. This results in an increase of T_c by more than a factor of two, $T_c/T_c^0 > 2$. Reflecting this dominance of BF coupling, we term this regime as the phase

of thermal-boson induced superconductivity. Naturally, the magnitude of n_B influences the enhancement of T_c . Driven by the last term in Eq. (5), T_c scales approximately linearly with n_B ; corresponding phase diagrams for different densities are presented in Ref. [46].

The boson mass is a further central parameter in determining the enhancement of T_c . Naively one might expect that a lighter mediator of interactions may be beneficial. For thermal-boson enhanced SC we find this not to be the case. As shown in Fig. 4, making the bosons heavier first enhances mediated interactions. Only for large boson mass the enhancement weakens and eventually recovers the original value of T_c^0 . Interestingly, a similar behavior of mixed boson-fermion systems was recently found in a study of the Fermi polaron problem where a significant mass imbalance leads to enhanced polaron dressing [59]. Attesting to the strength of the FRG, we note that without the self-consistent feedback between λ and g (Fig. 2(a)) one would obtain a monotonous, non-physical increase of the critical temperature extending into the limit $m_B/m_F \rightarrow \infty$ [46]. We also note that we do not include a polaronic renormalization of the fermionic mass in our analysis. However, as we consider a thermal bath such self-energy effects are expected to be small. Moreover, as fermions become heavier, the associated increase in the density of state may even further enhance T_c .

We have focused the discussion on the SC instability. To support our findings, we finally investigate the robustness of the SC transition with regards to a charge density wave (CDW) instability. Indeed, since g and λ correspond to effective in-medium scattering amplitudes, their mutual increase might hint at a tendency towards enhanced density-density correlations. To analyze the role of a potential CDW instability, we couple the action to source fields [31, 60–62] and monitor the divergence of associated vertex functions [46]. We find that

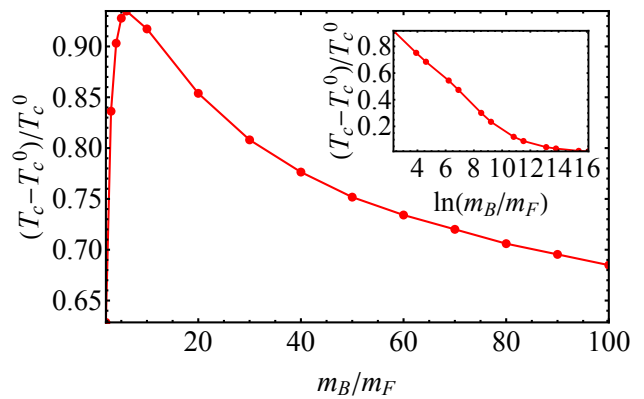


FIG. 4. **Mass scaling.** Enhancement of T_c relative to its bare value T_c^0 as function of the mass ratio m_B/m_F for $n_B/n_F = 0.1$, $(k_F a_{BF})^{-1} = -0.2$ and $(k_F a_{FF})^{-1} = -1.5$. Inset: Log-linear plot showing T_c up to large values of m_B/m_F .

within our truncation superconductivity always dominates. This finding is also in line with the fact that the boson dispersion in our model does not feature softening at a certain wavevector, which was a crucial ingredient to trigger CDW instabilities in previous work [13, 14].

Experimentally, our model can be realized in ultracold atomic mixtures featuring overlapping Feshbach resonances [63, 64]. The critical temperature can be measured in rotating paired superfluids [65] or by spectroscopy of the pairing gap [66, 67]. The predicted enhancement of correlations can be observed using atom-resolved techniques in continuum [68–70], and complementary momentum-space techniques [71]. In 2D materials, transport measurements are available as a direct probe of boson-enhanced superconductivity. Interestingly, the measurement of thermal-boson enhanced SC may provide a novel probe to observe the transition of excitonic insulators from the normal to the superfluid regime. Possible setups could include heterobilayers of TMDs coupled to a superconducting layer of (twisted) bilayer graphene which is in reach of current experimental techniques [72–75].

Conclusion.—We have shown that the coupling of a superconductor to a thermal boson bath can lead to a robust increase of the SC temperature T_c . In this way, T_c can reach more than twice of its bare value at moderate fermion coupling. For strongly-coupled fermion system, the enhancement becomes increasingly suppressed. As a result, the bound on $T_c/T_F \approx 0.16$ for the unitary Fermi gas remains robust. While we have mainly focused on three dimensions, we expect our results to be qualitatively applicable to the study of two-dimensional van der Waals materials. In this context, the extension of the present theory to include the physics of the Berezinskii–Kosterlitz–Thouless phase transition may allow to establish thermally-enhanced SC as a novel probe of the physics of excitonic insulators. A further interesting theoretical venue will be the full incorporation of three-body correlations and three-body loss which will be of particular importance in the regime of small boson masses which has not been focus of this work. Finally, the incorporation of a full BCS-BEC crossover [20, 23] will require the consideration of tightly bound fermions pairs which presents another interesting direction for future work.

Acknowledgements.—We thank Xin Chen, Jonas von Milczewski and Atac Imamoglu for inspiring discussions. E. V., M. S., and R. S. acknowledge support by the Deutsche Forschungsgemeinschaft under Germany’s Excellence Strategy EXC 2181/1 - 390900948 (the Heidelberg STRUCTURES Excellence Cluster), and CRC 1225 ISOQUANT, project-ID 273811115. R.S. was supported within the DFG scientific network ‘A(E)MP - Appearance of the Effective Mass in Polaron Models’ (Grant No. 569490025). E. D. acknowledges support from the Swiss National Science Foundation (SNSF) under Project 200021_212899 and Sinergia SNF_222792.

-
- [1] J. S. Hofmann, D. Chowdhury, S. A. Kivelson, and E. Berg, Heuristic bounds on superconductivity and how to exceed them, *npj quantum materials* **7**, 83 (2022).
 - [2] I. Esterlis, S. A. Kivelson, and D. J. Scalapino, A bound on the superconducting transition temperature, *npj quantum materials* **3**, 59 (2018).
 - [3] T. Hazra, N. Verma, and M. Randeria, Bounds on the superconducting transition temperature: Applications to twisted bilayer graphene and cold atoms, *Phys. Rev. X* **9**, 031049 (2019).
 - [4] C. A. Regal, M. Greiner, and D. S. Jin, Observation of resonance condensation of fermionic atom pairs, *Phys. Rev. Lett.* **92**, 040403 (2004).
 - [5] M. G. Ries, A. N. Wenz, G. Zürn, L. Bayha, I. Boettcher, D. Kedar, P. A. Murthy, M. Neidig, T. Lompe, and S. Jochim, Observation of pair condensation in the quasi-2d bec-bcs crossover, *Phys. Rev. Lett.* **114**, 230401 (2015).
 - [6] M. Oh, K. P. Nuckolls, D. Wong, R. L. Lee, X. Liu, K. Watanabe, T. Taniguchi, and A. Yazdani, Evidence for unconventional superconductivity in twisted bilayer graphene, *Nature* **600**, 240-245 (2021).
 - [7] D. Fausti, R. I. Tobey, N. Dean, S. Kaiser, A. Dienst, M. C. Hoffmann, S. Pyon, T. Takayama, H. Takagi, and A. Cavalleri, Light-induced superconductivity in a stripe-ordered cuprate, *Science* **331**, 189 (2011).
 - [8] M. Sidler, P. Back, O. Cotlet, A. Srivastava, T. Fink, M. Kroner, E. Demler, and A. Imamoglu, Fermi polaron-polaritons in charge-tunable atomically thin semiconductors, *Nature Physics* **13**, 255-261 (2017).
 - [9] M. Duda, X.-Y. Chen, A. Schindewolf, R. Bause, J. von Milczewski, R. Schmidt, I. Bloch, and X.-Y. Luo, Transition from a polaronic condensate to a degenerate fermi gas of heteronuclear molecules, *Nature Physics* **19**, 720-725 (2023).
 - [10] G. Cai, H. Ando, S. McCusker, and C. Chin, Fermion mediated pairing in the ruderman-kittel-kasuya-yosida to efimov transition regime, *Phys. Rev. Lett.* **136**, 083403 (2026).
 - [11] V. Ginzburg, On surface superconductivity, *Physics Letters* **13**, 101 (1964).
 - [12] W. A. Little, The exciton mechanism in superconductivity, *Journal of Polymer Science Part C: Polymer Symposia* **29**, 17 (1970).
 - [13] T. Enss and W. Zwerger, Superfluidity near phase separation in Bose-Fermi mixtures, *The European Physical Journal B* **68**, 383-389 (2009).
 - [14] O. Cotlet, S. Zeytinoglu, M. Sgrist, E. Demler, and A. Imamoglu, Superconductivity and other collective phenomena in a hybrid bose-fermi mixture formed by a polariton condensate and an electron system in two dimensions, *Phys. Rev. B* **93**, 054510 (2016).
 - [15] G. Wang, A. Chernikov, M. M. Glazov, T. F. Heinz, X. Marie, T. Amand, and B. Urbaszek, Colloquium: Excitons in atomically thin transition metal dichalcogenides, *Rev. Mod. Phys.* **90**, 021001 (2018).
 - [16] P. Massignan, R. Schmidt, G. E. Astrakharchik, A. Imamoglu, M. Zwierlein, J. J. Arlt, and G. M. Bruun, Polarons in atomic gases and two-dimensional semiconductors, *arXiv:2501.09618* (2025).
 - [17] F. P. Laussy, A. V. Kavokin, and I. A. Shelykh, Exciton-

- polariton mediated superconductivity, *Phys. Rev. Lett.* **104**, 106402 (2010).
- [18] M. Sun, A. V. Parafilo, V. M. Kovalev, and I. G. Savenko, Strong-coupling theory of condensate-mediated superconductivity in two-dimensional materials, *Phys. Rev. Res.* **3**, 033166 (2021).
- [19] A. Kumar, A. S. Patri, and T. Senthil, Unconventional superconductivity mediated by exciton density wave fluctuations, *Phys. Rev. Lett.* **135**, 266501 (2025).
- [20] J. von Milczewski, X. Chen, A. Imamoglu, and R. Schmidt, Superconductivity induced by strong electron-exciton coupling in doped atomically thin semiconductor heterostructures, *Phys. Rev. Lett.* **133**, 226903 (2024).
- [21] C. Zerba, C. Kuhlenkamp, A. Imamoglu, and M. Knap, Realizing topological superconductivity in tunable bose-fermi mixtures with transition metal dichalcogenide heterostructures, *Phys. Rev. Lett.* **133**, 056902 (2024).
- [22] C. Zerba, C. Kuhlenkamp, L. Mangeolle, and M. Knap, Tuning transport in solid-state bose-fermi mixtures by feshbach resonances, *Phys. Rev. Lett.* **134**, 126502 (2025).
- [23] V. Crépel, D. Guerci, J. Cano, J. H. Pixley, and A. Millis, Topological superconductivity in doped magnetic moiré semiconductors, *Phys. Rev. Lett.* **131**, 056001 (2023).
- [24] D. S. Antonenko and M. A. Skvortsov, Suppression of superconductivity in disordered films: Interplay of two-dimensional diffusion and three-dimensional ballistics, *JETP Letters* **112**, 428-436 (2020).
- [25] R. A. Smith and V. Ambegaokar, Effect of magnetic impurities on suppression of the transition temperature in disordered superconductors, *Phys. Rev. B* **62**, 5913 (2000).
- [26] A. Ślebarski, M. Fijałkowski, P. Zajdel, M. M. Maška, J. Deniszczyk, M. Zubko, O. Pavlosiuk, K. Sasmal, and M. B. Maple, Enhancing superconductivity of lu 5 rh 6 sn 18 by atomic disorder, *Phys. Rev. B* **102**, 054514 (2020).
- [27] A. T. Rømer, P. J. Hirschfeld, and B. M. Andersen, Raising the critical temperature by disorder in unconventional superconductors mediated by spin fluctuations, *Phys. Rev. Lett.* **121**, 027002 (2018).
- [28] M. Leroux, V. Mishra, J. P. C. Ruff, H. Claus, M. P. Smylie, C. Opagiste, P. Rodière, A. Kayani, G. D. Gu, J. M. Tranquada, W.-K. Kwok, Z. Islam, and U. Welp, Disorder raises the critical temperature of a cuprate superconductor, *Proceedings of the National Academy of Sciences* **116**, 10691 (2019).
- [29] K. Aoki, Introduction to the nonperturbative renormalization group and its recent applications, *Int. J. Mod. Phys. B* **14**, 1249 (2000).
- [30] C. Bagnuls and C. Bervillier, Exact renormalization group equations. An Introductory review, *Phys. Rept.* **348**, 91 (2001).
- [31] M. Salmhofer and C. Honerkamp, Fermionic renormalization group flows: Technique and theory, *Prog. Theor. Phys.* **105**, 1 (2001).
- [32] J. Berges, N. Tetradis, and C. Wetterich, Nonperturbative renormalization flow in quantum field theory and statistical physics, *Phys. Rept.* **363**, 223 (2002).
- [33] J. M. Pawłowski, Aspects of the functional renormalisation group, *Annals Phys.* **322**, 2831 (2007).
- [34] W. Metzner, M. Salmhofer, C. Honerkamp, V. Meden, and K. Schonhammer, Functional renormalization group approach to correlated fermion systems, *Rev. Mod. Phys.* **84**, 299 (2012).
- [35] C. Wetterich, Exact evolution equation for the effective potential, *Physics Letters B* **301**, 90-94 (1993).
- [36] H. Gies, Introduction to the functional rg and applications to gauge theories, in *Renormalization Group and Effective Field Theory Approaches to Many-Body Systems*, edited by A. Schwenk and J. Polonyi (Springer Berlin Heidelberg, Berlin, Heidelberg, 2012) pp. 287–348.
- [37] M. M. Parish, The bcs-bec crossover, in *Quantum Gas Experiments*, Chap. Chapter 9, pp. 179–197.
- [38] M. Randeria and E. Taylor, Crossover from bardeen-cooper-schrieffer to bose-einstein condensation and the unitary fermi gas, *Annual Review of Condensed Matter Physics* **5**, 209 (2014).
- [39] W. Zwerger, *The BCS-BEC crossover and the unitary Fermi gas*, Vol. 836 (Springer Science & Business Media, 2011).
- [40] P. Nozieres and S. Schmitt-Rink, Bose condensation in an attractive fermion gas: From weak to strong coupling superconductivity, *J. Low Temp. Phys.* **59**, 195-211 (1985).
- [41] M. Randeria, J.-M. Duan, and L.-Y. Shieh, Superconductivity in a two-dimensional fermi gas: Evolution from cooper pairing to bose condensation, *Phys. Rev. B* **41**, 327 (1990).
- [42] J. Bardeen, L. N. Cooper, and J. R. Schrieffer, Theory of superconductivity, *Phys. Rev.* **108**, 1175 (1957).
- [43] A. J. Leggett, Diatomic molecules and cooper pairs, in *Modern Trends in the Theory of Condensed Matter*, edited by A. Pekalski and J. A. Przystawa (Springer Berlin Heidelberg, Berlin, Heidelberg, 1980) pp. 13–27.
- [44] D. M. Eagles, Possible pairing without superconductivity at low carrier concentrations in bulk and thin-film superconducting semiconductors, *Phys. Rev.* **186**, 456 (1969).
- [45] R. Schmidt, *From few-to many-body physics with ultracold atoms*, Ph.D. thesis, Technische Universität München (2013).
- [46] See Supplemental Material for further information.
- [47] Z. Yan, P. B. Patel, B. Mukherjee, R. J. Fletcher, J. Struck, and M. W. Zwierlein, Boiling a unitary fermi liquid, *Phys. Rev. Lett.* **122**, 093401 (2019).
- [48] Analogously to the fermions the bosonic Green's function is regulated by a sharp regulator $G_B^c(\mathbf{p}, \omega) = G_B(\mathbf{p}, \omega)\theta(p - k)$.
- [49] E. Burovski, N. Prokof'ev, B. Svistunov, and M. Troyer, Critical temperature and thermodynamics of attractive fermions at unitarity, *Phys. Rev. Lett.* **96**, 160402 (2006).
- [50] E. Burovski, E. Kozik, N. Prokof'ev, B. Svistunov, and M. Troyer, Critical temperature curve in bec-bcs crossover, *Phys. Rev. Lett.* **101**, 090402 (2008).
- [51] O. Goulko and M. Wingate, Thermodynamics of balanced and slightly spin-imbalanced fermi gases at unitarity, *Phys. Rev. A* **82**, 053621 (2010).
- [52] Based on findings on polaron physics and induced superconductivity in cold atoms and 2D materials [16, 20], we expect our results to qualitatively apply also for 2D systems.
- [53] C. Chin, R. Grimm, P. Julienne, and E. Tiesinga, Feshbach resonances in ultracold gases, *Rev. Mod. Phys.* **82**, 1225 (2010).
- [54] The BCS weak-coupling gap and the phase-shift are calculated using the relations $\Delta_0 = 1.764T_c^0$ and $\delta_{BF} = \text{arccot}(-1/(k_F a_{BF}))$.
- [55] C. Fey, P. Schmelcher, A. Imamoglu, and R. Schmidt, Theory of exciton-electron scattering in atomically thin

- semiconductors, *Phys. Rev. B* **101**, 195417 (2020).
- [56] S. S. Kumar, B. C. Mulkerin, A. Tiene, F. M. Marchetti, M. M. Parish, and J. Levinsen, Efficient calculation of trion energies in monolayer transition metal dichalcogenides, *Phys. Rev. B* **111**, 085404 (2025).
- [57] M. Wagner, R. Oldziejewski, F. Rose, V. Köder, C. Kuhlenskamp, A. İmamoğlu, and R. Schmidt, Feshbach resonances in exciton–charge-carrier scattering in semiconductor bilayers, *Phys. Rev. Lett.* **134**, 076903 (2025).
- [58] H. Mitzenzwey, A. Knorr, and T. Deilmann, Coulomb interaction in atomically thin semiconductors and density-independent exciton-scattering processes (2026), [arXiv:2602.13763](https://arxiv.org/abs/2602.13763).
- [59] X. Chen, E. Dizer, E. R. Rodríguez, and R. Schmidt, Mass-gap description of heavy impurities in fermi gases, *Phys. Rev. Lett.* **135**, 193401 (2025).
- [60] C. J. Halboth and W. Metzner, Renormalization-group analysis of the two-dimensional hubbard model, *Phys. Rev. B* **61**, 7364 (2000).
- [61] W. Metzner, M. Salmhofer, C. Honerkamp, V. Meden, and K. Schönhammer, Functional renormalization group approach to correlated fermion systems, *Rev. Mod. Phys.* **84**, 299 (2012).
- [62] L. Désoppi, N. Dupuis, and C. Bourbonnais, Functional renormalization group for fermions on a one dimensional lattice at arbitrary filling, *SciPost Phys.* **17**, 054 (2024).
- [63] J. Goldwin, S. Inouye, M. L. Olsen, B. Newman, B. D. DePaola, and D. S. Jin, Measurement of the interaction strength in a bose-fermi mixture with ^{87}Rb and ^{40}K , *Phys. Rev. A* **70**, 021601 (2004).
- [64] G. Roati, F. Riboli, G. Modugno, and M. Inguscio, Fermi-bose quantum degenerate ^{40}K – ^{87}Rb mixture with attractive interaction, *Phys. Rev. Lett.* **89**, 150403 (2002).
- [65] M. W. Zwierlein, J. R. Abo-Shaeer, A. Schirotzek, C. H. Schunck, and W. Ketterle, Vortices and superfluidity in a strongly interacting fermi gas, *Nature* **435**, 1047-1051 (2005).
- [66] C. Chin, M. Bartenstein, A. Altmeyer, S. Riedl, S. Jochim, J. H. Denschlag, and R. Grimm, Observation of the pairing gap in a strongly interacting fermi gas, *Science* **305**, 1128 (2004).
- [67] J. T. Stewart, J. P. Gaebler, and D. S. Jin, Using photoemission spectroscopy to probe a strongly interacting fermi gas, *Nature* **454**, 744-747 (2008).
- [68] R. Yao, S. Chi, M. Wang, R. J. Fletcher, and M. Zwierlein, Measuring pair correlations in bose and fermi gases via atom-resolved microscopy, *Phys. Rev. Lett.* **134**, 183402 (2025).
- [69] T. de Jongh, J. Verstraten, M. Dixmierias, C. Daix, B. Peaudecerf, and T. Yefsah, Quantum gas microscopy of fermions in the continuum, *Phys. Rev. Lett.* **134**, 183403 (2025).
- [70] J. Xiang, E. Cruz-Colón, C. C. Chua, W. R. Milner, J. de Hond, J. F. Fricke, and W. Ketterle, In situ imaging of the thermal de broglie wavelength in an ultracold bose gas, *Phys. Rev. Lett.* **134**, 183401 (2025).
- [71] T. Jelten, J. M. McNamara, W. Hogervorst, W. Vassen, V. Krachmalnicoff, M. Schellekens, A. Perrin, H. Chang, D. Boiron, A. Aspect, and C. I. Westbrook, Comparison of the Hanbury Brown-Twiss effect for bosons and fermions, *Nature* **445**, 402-405 (2007).
- [72] Y. Cao, V. Fatemi, S. Fang, K. Watanabe, T. Taniguchi, E. Kaxiras, and P. Jarillo-Herrero, Unconventional superconductivity in magic-angle graphene superlattices, *Nature* **556**, 43-50 (2018).
- [73] P. Rivera, K. L. Seyler, H. Yu, J. R. Schaibley, J. Yan, D. G. Mandrus, W. Yao, and X. Xu, Valley-polarized exciton dynamics in a 2d semiconductor heterostructure, *Science* **351**, 688 (2016).
- [74] A. Inbar, J. Birkbeck, J. Xiao, T. Taniguchi, K. Watanabe, B. Yan, Y. Oreg, A. Stern, E. Berg, and S. Ilani, The quantum twisting microscope, *Nature* **614**, 682 (2023).
- [75] L. Ma, P. X. Nguyen, Z. Wang, Y. Zeng, K. Watanabe, T. Taniguchi, A. H. MacDonald, K. F. Mak, and J. Shan, Strongly correlated excitonic insulator in atomic double layers, *Nature* **598**, 585-589 (2021).

Supplemental Material for 'Enhancing superconductivity using thermal bosons'

Ekaterina Vlasiuk,¹ Manfred Salmhofer,¹ Eugene Demler,² and Richard Schmidt¹

¹*Institute for Theoretical Physics, Heidelberg University, 69120 Heidelberg, Germany*

²*Institute for Theoretical Physics, ETH Zürich, 8093 Zürich, Switzerland*

In this supplemental material we provide further information and details on our calculations leading to the results presented in the main text of our work. Specifically, in Sec. I we show how the well-known BCS results are obtained within the Functional Renormalization Group (FRG) framework, and discuss the Gorkov-Melik-Barkhudarov correction to BCS theory. In Secs. II and III we present the integral expression entering the RG flow equations for the Bose-Fermi mixture, and we discuss the associated initial conditions. In Sec. IV we present the fixed point diagram in the vacuum limit, while in Sec. V we discuss the derivation of an effective weak-coupling theory for the fermions following integrating out the bosonic degrees of freedom. In Sec. VI we present phase diagrams of enhanced/induced superconductivity in Bose-Fermi mixtures for various density ratios between bosons and fermions. In Sec. VII we discuss the nonphysical behaviour of the critical superconducting temperature when the problem is solved in a non-self-consistent approach. Finally, in Sec. VIII we discuss and analyse the role of a potential charge density wave instability.

I. BCS THEORY FROM THE FUNCTIONAL RENORMALIZATION GROUP AND GORKOV-MELIK-BARKHUDAROV (GBM) CORRECTION

The well-known results from BCS theory can be obtained from the Functional Renormalization Group (FRG) for the purely fermionic system by keeping only the first diagram in Fig. 2(a) of the main text. This leads to the flow equation

$$\partial_k g_k = -g_k^2 \tilde{\partial}_k \int_Q G_F^c(Q) G_F^c(-Q). \quad (S1)$$

In the weak coupling limit, $k_F a \rightarrow 0^-$, one then obtains [1]

$$T_c^0 = \frac{8e^\gamma}{\pi e^2} e^{-\frac{\pi}{2} \left| \frac{1}{k_F a} \right|}, \quad (S2)$$

recovering the BCS result. In the unitary limit $1/k_F a \rightarrow 0$ one arrives at the well-known result $T_c^0/E_F \approx 0.5$ (see the dashed blue curve in Fig. 3(a)) [2], which can also be obtained using a non-self-consistent T-matrix approach.

For the transparency and simple analysis of our results we neglect the Gorkov-Melik-Barkhudarov (GMB) correction in the main text. One generally obtains the GMB correction following the FRG procedure outlined in the main text. The associated flow equation for the pure fermionic model including the GMB correction (for its diagrammatic representation, see Fig. S1) is given by

$$\partial_k g_k = -g_k^2 I_{BCS} - g_k^2 I_2. \quad (S3)$$

The GMB correction would overall lower the critical temperature in comparison to pure BCS theory but it would not qualitatively impact the mechanism leading to the enhancement of T_c by thermal bosons.

II. INTEGRAL EXPRESSIONS

Here we provide the integral expressions entering the flow equations (5)-(6) of the main text. They are given by

$$I_{BCS} = \tilde{\partial}_k \int_Q G_F^c(Q) G_F^c(-Q) = -\frac{m_F}{2\pi^2 k} \tanh \left[\frac{k^2}{4m_F T} \right] \left\{ \theta \left(\mu_F - \frac{k^2}{2m_F} \right) \sqrt{2m_F \mu_F - k^2} + \sqrt{2m_F \mu_F + k^2} \right\}, \quad (S4)$$

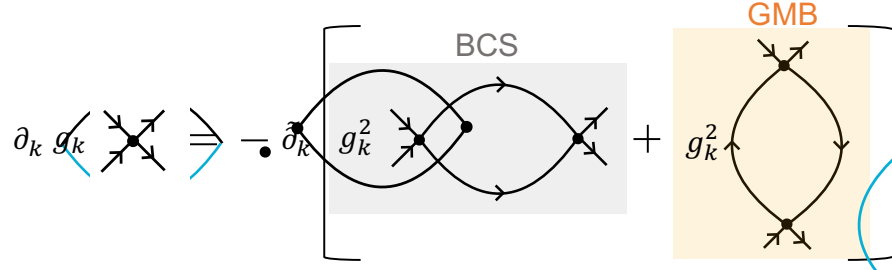


FIG. S1 Flow equation for the flowing coupling constant between fermions g_k in the pure fermionic theory with the inclusion of Gorkov-Melik-Barkhudarov correction.

and

$$I_1 = \frac{1}{2} \int_{-1}^1 d \cos \varphi \tilde{\partial}_k \int_Q G_B^c(Q) G_B^c(Q + L_3 - L_2) = -\frac{k^2 m_B}{2\pi^2 k_F^2} \left[\left(1 + \frac{k_F}{k}\right) \ln \left(1 + \frac{k_F}{k}\right) + \left(1 - \frac{k_F}{k}\right) \ln \left|1 - \frac{k_F}{k}\right| \right] n_B \left(\frac{k^2}{2m_B} - \mu_B\right), \quad (\text{S5})$$

where $\varphi = \angle(l_2, l_3)$. Moreover,

$$I_2 = \frac{1}{2} \int_{-1}^1 d \cos \varphi \tilde{\partial}_k \int_Q G_F^c(Q) G_F^c(Q + L_1 - L_4) = \frac{m_F k \sqrt{2m_F \mu_F + k^2}}{2\pi^2 k_F^2} \times \left[\left(1 + \frac{k_F}{\sqrt{2m_F \mu_F + k^2}}\right) \ln \left(1 + \frac{k_F}{\sqrt{2m_F \mu_F + k^2}}\right) + \left(1 - \frac{k_F}{\sqrt{2m_F \mu_F + k^2}}\right) \ln \left|1 - \frac{k_F}{\sqrt{2m_F \mu_F + k^2}}\right| \right] n_F \left(\frac{k^2}{2m_F}\right) + \frac{m_F k \sqrt{2m_F \mu_F - k^2}}{2\pi^2 k_F^2} \left[\left(1 + \frac{k_F}{\sqrt{2m_F \mu_F - k^2}}\right) \ln \left(1 + \frac{k_F}{\sqrt{2m_F \mu_F - k^2}}\right) + \left(1 - \frac{k_F}{\sqrt{2m_F \mu_F - k^2}}\right) \ln \left|1 - \frac{k_F}{\sqrt{2m_F \mu_F - k^2}}\right| \right] n_F \left(-\frac{k^2}{2m_F}\right) \theta \left(\mu_F - \frac{k^2}{2m_F}\right), \quad (\text{S6})$$

where $\varphi = \angle(l_1, l_4)$, and

$$I_3 = \int_Q G_F^c(-Q + L_4 + L_3) G_B^c(Q) = \int_Q G_F^c(-Q) G_B^c(Q) = -\frac{k \sqrt{2m_F \mu_F + k^2}}{2\pi^2} \left[\frac{n_F \left(-\frac{k^2}{2m_F}\right) + n_B \left(\frac{k^2}{2m_B} + \frac{m_F}{m_B} \mu_F - \mu_B\right)}{\left(\frac{1}{2} \left(\frac{1}{m_B} + \frac{1}{m_F}\right) (2m_F \mu_F + k^2) - \mu_B - \mu_F\right)^2 + (\pi T)^2} \right] \times \left[\frac{1}{2} \left(\frac{1}{m_B} + \frac{1}{m_F}\right) (2m_F \mu_F + k^2) - \mu_B - \mu_F \right] - \frac{k^2}{2\pi^2} \left[\frac{n_F \left(-\frac{k^2}{2m_F} + \mu_F\right) + n_B \left(\frac{k^2}{2m_B} - \mu_B\right)}{\left(\frac{1}{2} \left(\frac{1}{m_B} + \frac{1}{m_F}\right) k^2 - \mu_B - \mu_F\right)^2 + (\pi T)^2} \right] \left[\frac{1}{2} \left(\frac{1}{m_B} + \frac{1}{m_F}\right) k^2 - \mu_B - \mu_F \right] \theta \left(\mu_F - \frac{k^2}{m_F}\right) \quad (\text{S7})$$

$$\begin{aligned}
I_4 &= -\frac{1}{2} \int_{-1}^1 d \cos \varphi \int_Q G_F^c(Q + L_4 - L_2) G_B^c(Q) \\
&= -\frac{1}{2} \int_{-1}^1 dy \left\{ \left[\frac{m_B k}{4\pi^2 p} n_F \left(\frac{q^2}{2m_F} - \mu_F \right) \ln \left| \frac{-\frac{qp}{m_B} + \frac{q^2}{2} \left(\frac{1}{m_B} - \frac{1}{m_F} \right) + \frac{p^2}{2m_B} + \mu_F - \mu_B}{+\frac{qp}{m_B} + \frac{q^2}{2} \left(\frac{1}{m_B} - \frac{1}{m_F} \right) + \frac{p^2}{2m_B} + \mu_F - \mu_B} \right| \right. \right. \\
&\quad \left. \left. + \frac{m_F k}{4\pi^2 p} n_B \left(\frac{q^2}{2m_B} - \mu_B \right) \ln \left| \frac{-\frac{qp}{m_F} + \frac{q^2}{2} \left(\frac{1}{m_B} - \frac{1}{m_F} \right) - \frac{p^2}{2m_F} + \mu_F - \mu_B}{+\frac{qp}{m_F} + \frac{q^2}{2} \left(\frac{1}{m_B} - \frac{1}{m_F} \right) - \frac{p^2}{2m_F} + \mu_F - \mu_B} \right| \right] \right. \\
&\quad \left. + \left[\frac{m_B k}{4\pi^2 p} n_F \left(\frac{k^2}{2m_F} - \mu_F \right) \ln \left| \frac{-\frac{kp}{m_B} + \frac{k^2}{2} \left(\frac{1}{m_B} - \frac{1}{m_F} \right) + \frac{p^2}{2m_B} + \mu_F - \mu_B}{+\frac{kp}{m_B} + \frac{k^2}{2} \left(\frac{1}{m_B} - \frac{1}{m_F} \right) + \frac{p^2}{2m_B} + \mu_F - \mu_B} \right| \right. \right. \\
&\quad \left. \left. + \frac{m_F k}{4\pi^2 p} n_B \left(\frac{k^2}{2m_B} - \mu_B \right) \ln \left| \frac{-\frac{kp}{m_F} + \frac{k^2}{2} \left(\frac{1}{m_B} - \frac{1}{m_F} \right) - \frac{p^2}{2m_F} + \mu_F - \mu_B}{+\frac{kp}{m_F} + \frac{k^2}{2} \left(\frac{1}{m_B} - \frac{1}{m_F} \right) - \frac{p^2}{2m_F} + \mu_F - \mu_B} \right| \right] \theta \left(\mu_F - \frac{k^2}{m_F} \right) \right\}, \tag{S8}
\end{aligned}$$

where $q = \sqrt{2m_F \mu_F + k^2}$, $p = \sqrt{2k_F \sqrt{1-y}}$.

In these equations L_3 and L_4 denote incoming external momenta and frequencies of the scattering fermions while L_1 and L_2 are outgoing external momenta and frequencies. In the above derivation we considered the low-energy physics by projecting the external momenta onto the Fermi surface at zero center-of-mass momentum, and we assumed that the chemical potential of fermions μ_F is positive, which is a valid assumption for low enough temperatures. Similar to previous studies [3], we ignored the external momentum dependence in the regulator function in favor of obtaining analytical results, as this approach does not influence the results on the qualitative level.

III. INITIAL CONDITIONS

For the solution of the flow equations one has to set the initial conditions. This means that one has to find some limit in which the solution of the flow equations is known. This is achieved by considering the solution at the UV scale, where it is fully governed by short-distance, and thus two-body scattering physics. In the two-body limit (also called ‘vacuum limit’), the chemical potentials and temperature are set to zero ($\mu_F = \mu_B = 0$, $T = 0$). From the flow equations in this limit one obtains

$$\begin{aligned}
g_{k=\Lambda} &= \left(\frac{m_F}{4\pi a_{FF}} - \frac{m_F}{2\pi^2} \Lambda \right)^{-1}, \\
\lambda_{k=\Lambda} &= \left(\frac{1}{2\pi a_{BF}} \frac{m_B m_F}{m_B + m_F} - \frac{1}{\pi^2} \frac{m_B m_F}{m_B + m_F} \Lambda \right)^{-1}, \tag{S9}
\end{aligned}$$

where we used that in the two-body limit $g_{k=0} = 4\pi a_{FF}/\mu_{FF}$ and $\lambda_{k=0} = 2\pi a_{BF}(m_B + m_F)/(m_B m_F)$ as the flowing constants are the zero-energy two-body T-matrices which in its turn are connected to the scattering amplitudes and the scattering wavelengths. We utilize these expressions as the initial conditions for the flow equations.

IV. FIXED POINTS DIAGRAM IN THE VACUUM LIMIT

The tendencies in the behaviour of the flowing coupling constants can be already seen in the vacuum limit at vanishing densities and temperature. Here the flow equations are given by

$$\begin{aligned}
\partial_k \tilde{g}_k &= \frac{m_F}{2\pi^2} \tilde{g}_k^2 + \tilde{g}_k, \\
\partial_k \tilde{\lambda}_k &= \frac{1}{\pi^2} \frac{m_B m_F}{m_B + m_F} \tilde{\lambda}_k^2 + \tilde{\lambda}_k, \tag{S10}
\end{aligned}$$

where we use rescaled quantities $k = \Lambda e^t$, $\tilde{g} = gk$ and $\tilde{\lambda} = \lambda k$. The RG diagram in Fig. S2 shows the strong coupling fixed points and instability towards fermion-fermion and fermion-boson pairing, i.e. $g \rightarrow -\infty$ $\lambda \rightarrow -\infty$, which drives the physics described in this work.

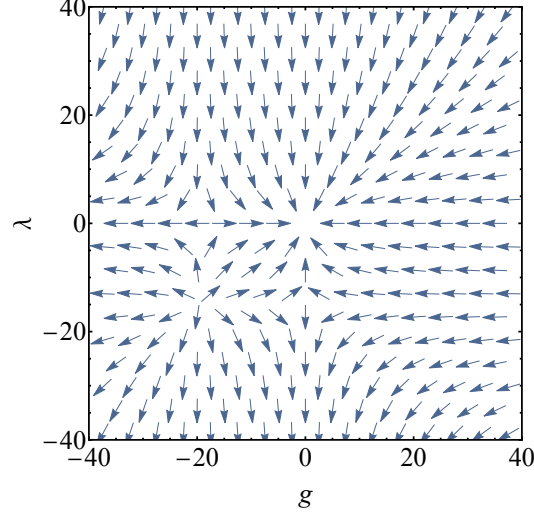


FIG. S2 Fixed points diagram of the RG flow equations in the vacuum limit for $K^{40}\text{-Rb}^{87}$ mixture. The arrows show the direction towards the IR limit.

V. EFFECTIVE THEORY IN THE WEAK COUPLING LIMIT

The action is quadratic in bosonic fields. Thus it is possible to integrate the bosons out exactly, which, when performed in the limit of the weak-coupling between bosons and fermions, leads to an analytical understanding of boson-mediated interactions. In particular it provides a solid check of the character of the induced interaction. Of course, this approach will not allow to reach the strong-coupling regime, as keeping only lowest-order induced interactions in this approach, one cannot account for the mutual influence between different scattering channels which is crucial, for instance, for uncovering the nontrivial mass dependence of the critical temperature discussed in the main text. To obtain the effective weak-coupling theory, we start with the action for the Bose-Fermi mixture

$$\begin{aligned}
S = & \sum_{\sigma=\uparrow,\downarrow} \int_P \psi_{\sigma}^*(P) \left(i\omega - \frac{p^2}{2m_F} + \mu_F \right) \psi_{\sigma}(P) + \int_P \varphi^*(P) \left(i\omega - \frac{p^2}{2m_B} + \mu_B \right) \varphi(P) \\
& + g_k \int_{Q,P,P'} \psi_{\uparrow}^*(P+Q) \psi_{\downarrow}^*(P'-Q) \psi_{\downarrow}(P') \psi_{\uparrow}(P) \\
& + \sum_{\sigma=\uparrow,\downarrow} \lambda^{\sigma} \int_{Q,P,K'} \psi_{\sigma}^*(P+Q) \varphi^*(K'-Q) \varphi(K') \psi_{\sigma}(P).
\end{aligned} \tag{S11}$$

The partition function is then given by

$$\begin{aligned}
Z = & \int D[\psi_{\uparrow}, \psi_{\uparrow}^*, \psi_{\downarrow}, \psi_{\downarrow}^*, \varphi, \varphi^*] \exp \left(-S_F[\psi_{\uparrow}, \psi_{\uparrow}^*, \psi_{\downarrow}, \psi_{\downarrow}^*] - \sum_{KK'} \varphi^*(K) K_{KK'} [\psi_{\uparrow}, \psi_{\uparrow}^*, \psi_{\downarrow}, \psi_{\downarrow}^*] \varphi(K') \right), \\
& K[\psi_{\uparrow}, \psi_{\uparrow}^*, \psi_{\downarrow}, \psi_{\downarrow}^*]_{KK'} = G_B^{-1} \delta_{K,K'} + \sum_{\sigma=\uparrow,\downarrow} \lambda^{\sigma} (N_{F\sigma})_{KK'}, \\
& (N_{F\sigma})_{KK'} = \int_Q n_{F\sigma}(Q) \delta_{K',K+Q}, \quad n_{F\sigma}(Q) = \int_P \psi_{\sigma}^*(P+Q) \psi_{\sigma}(P).
\end{aligned} \tag{S12}$$

We now perform the functional integration, followed by the expansion of the result

$$\int D[\varphi, \varphi^*] \exp \left(- \sum_{KK'} \varphi^*(K) K_{KK'} [\psi_{\uparrow}, \psi_{\uparrow}^*, \psi_{\downarrow}, \psi_{\downarrow}^*] \varphi(K') \right) = \frac{C}{\det K}, \quad C > 0, \tag{S13}$$

$$\det K = \exp(\text{Tr} \ln K) = \exp \left[\text{Tr} \ln G_B^{-1} + \text{Tr} \ln \left(1 + \sum_{\sigma=\uparrow,\downarrow} \lambda^\sigma N_{F\sigma} G_B \right) \right] \quad (\text{S14})$$

$$\approx \exp \left[\text{Tr} \ln G_B^{-1} + \text{Tr} \left(\sum_{\sigma=\uparrow,\downarrow} \lambda^\sigma N_{F\sigma} G_B \right) - \frac{1}{2} \text{Tr} \left(\sum_{\sigma=\uparrow,\downarrow, \sigma'=\uparrow,\downarrow} \lambda^\sigma \lambda^{\sigma'} N_{F\sigma} G_B N_{F\sigma'} G_B \right) \right].$$

Taking the definition of the effective action $Z = \int D[\psi_\uparrow, \psi_\uparrow^*, \psi_\downarrow, \psi_\downarrow^*] \exp(-S_{\text{eff}})$ into account we obtain

$$S_{\text{eff}} = S_F[\psi_\uparrow, \psi_\uparrow^*, \psi_\downarrow, \psi_\downarrow^*] + \text{Tr} \ln G_B^{-1} + \text{Tr} \left(\sum_{\sigma=\uparrow,\downarrow} \lambda^\sigma N_{F\sigma} G_B \right) - \frac{1}{2} \text{Tr} \left(\sum_{\sigma=\uparrow,\downarrow, \sigma'=\uparrow,\downarrow} \lambda^\sigma \lambda^{\sigma'} N_{F\sigma} G_B N_{F\sigma'} G_B \right). \quad (\text{S15})$$

One can see that the interaction term which is quadratic in λ is attractive since

$$\text{Tr}(N_F G_B N_F G_B) = \int dK f(K) n_F(K) n_F(-K), \quad f(K) = \int dK_1 G_B(K_1) G_B(K_1 + K) > 0. \quad (\text{S16})$$

This result agrees with the FRG calculation in the main text, namely, the $\lambda_k^\uparrow \lambda_k^\downarrow$ term in Eq. (5) is attractive.

We note that in the reverse case where the interaction between fermions is absent one can obtain an effective induced interaction between bosons by performing the same procedure as above by integrating out the fermionic fields. The difference is that in Eq. (S13) the determinant would be in the numerator, and the sign of the function analogous to $f(K)$ in Eq. (S16), but with fermionic propagators, would be opposite. As a result, the quadratic term in the effective bosonic action would also be attractive. When extending the truncation of our FRG approach to featuring induced bosonic interactions we would thus also find induced attraction between bosons. The resulting density collapse of the system would, however, be prevented by a sufficiently strong two-body repulsion between bosons.

VI. PHASE DIAGRAMS FOR DIFFERENT DENSITIES

In this section we present the phase diagrams of enhanced/induced superconductivity in a $\text{K}^{40}\text{-Rb}^{87}$ Bose-Fermi mixture for different boson densities n_B . The results are shown in Fig. S3 which are obtained analogously to the results shown in the main text.

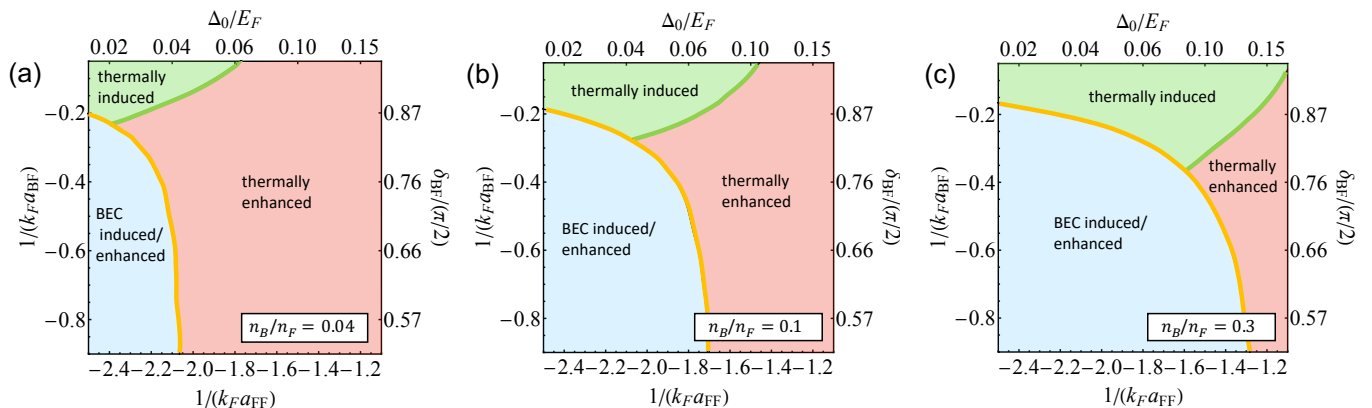


FIG. S3 Phase diagram of boson-modified superconductivity for a $\text{K}^{40}\text{-Rb}^{87}$ Bose-Fermi mixture for the different densities: (a) $n_B/n_F = 0.04$, (b) $n_B/n_F = 0.1$, (c) $n_B/n_F = 0.3$. The border between the thermally induced and thermally enhanced superconductivity regions is defined by the condition $T_c = 2T_c^0$.

VII. NONPHYSICAL BEHAVIOUR OF THE CRITICAL TEMPERATURE WITHIN THE NON-SELF-CONSISTENT SOLUTION OF THE FLOW EQUATIONS

When approaching the solution of RG equations in a non-selfconsistent way, i.e without the feedback of the renormalization of the boson-fermion interaction vertex, one encounters a monotonous increase of the superconducting

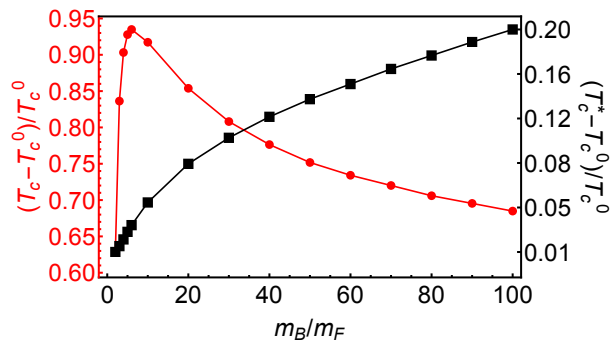


FIG. S4 The dependence of the critical superconducting temperature T_c on the mass ratio between bosons and fermions m_B/m_F with (red curve) and without (black curve) having a feedback of λ -vertex, $\lambda = -1$. Parameters are $n_B/n_F = 0.1$, $k_F a_{BF} = -5$, $k_F a_{FF} = -2/3$.

critical temperature with the bosonic mass. In other words, if one keeps the λ -vertex constant in the flow equation for g (see Fig. 2(a) in the main text), one obtains a nonphysical growth of the critical temperature with the mass of bosons in the limit $m_B/m_F \rightarrow \infty$, which is shown in Fig. S4).

VIII. CHARGE DENSITY WAVE INSTABILITY

In order to study if the system is prone to a CDW order instability we compare the responses of the system to external fields representing CDW and superconducting order parameters. To this end we add the source terms

$$\begin{aligned} \Gamma_{source}^{CDW} &= \int_{K,Q} Z_k^{ch} h(Q) \{ \psi_{\uparrow}^*(K+Q) \psi_{\uparrow}(K) + \psi_{\downarrow}^*(K+Q) \psi_{\downarrow}(K) \}, \\ \Gamma_{source}^s &= \int_K Z_k^s J [\psi_{\downarrow}^*(K) \psi_{\uparrow}^*(-K) - \psi_{\uparrow}^*(K) \psi_{\downarrow}^*(-K)] + \text{h.c.} \end{aligned} \quad (\text{S17})$$

to our truncation given by Eq. (4) of the main text. Comparing the rates at which the vertexes Z_k^{ch} and Z_k^s approach infinity, shows which order parameter tends to dominate. The flow equations for Z_k^s and Z_k^{ch} , which are dependent on the difference of external momenta, e.g. the charge density wave ordering vector, are given by (for a related discussion see, e.g., Ref. [3])

$$\begin{aligned} \frac{\partial Z_k^{ch}}{\partial k} &= Z_k^{ch} g_k I_2, \\ \frac{\partial Z_k^s}{\partial k} &= Z_k^s g_k I_{BCS} \end{aligned} \quad (\text{S18})$$

with the initial conditions $Z_k^{ch}(0) = 1$ and $Z_k^s(0) = 1$. Their diagrammatic representation is shown in Fig. S5. These equations are solved together with Eqs. (5,6) of the main text.

As I_{BCS} is bigger than I_2 , the vertex corresponding to coupling to the superconducting order parameter approaches infinity faster. Thus superconductivity will always dominate over the charge density wave state within our model.

$$\begin{aligned}
 \partial_k Z_k^{ch} \text{---} \text{---} \text{---} \text{---} &= \tilde{\partial}_k Z_k^{ch} g_k \text{---} \text{---} \text{---} \text{---} \\
 \partial_k Z_k^s \text{---} \text{---} \text{---} \text{---} &= \tilde{\partial}_k Z_k^s g_k \text{---} \text{---} \text{---} \text{---}
 \end{aligned}$$

FIG. S5 Diagrammatic representation of the flow equations of the vertexes Z_k^{ch} and Z_k^s given by Eq. (S18). g_k is the flowing four-fermion point-like coupling constant.

-
- [1] R. Schmidt, *From few-to many-body physics with ultracold atoms*, Ph.D. thesis, Technische Universität München (2013).
 - [2] C. A. R. Sá de Melo, M. Randeria, and J. R. Engelbrecht, Crossover from bcs to bose superconductivity: Transition temperature and time-dependent ginzburg-landau theory, *Phys. Rev. Lett.* **71**, 3202 (1993).
 - [3] L. Désoppi, N. Dupuis, and C. Bourbonnais, Functional renormalization group for fermions on a one dimensional lattice at arbitrary filling, *SciPost Phys.* **17**, 054 (2024).